Complex Robot Training Tasks through Bootstrapping System Identification

Otar Akanyeti[1], Ulrich Nehmzow[2], and S A Billings
[1]Dept Computer Science, University of Essex
[2]Dept Computer Science, University of Ulster, Ireland

Department of Automatic Control and Systems Engineering
The University of Sheffield, Sheffield, S1 3JD, UK

Research Report No. 982

July 2008

Complex Robot Training Tasks through Bootstrapping System Identification

Otar Akanyeti[1], Ulrich Nehmzow[2], and Steve Billings[3]

***Abstract*— Many sensor-motor competences in mobile robotics applications exhibit complex, non-linear characteristics. Previous research has shown that polynomial NARMAX models can learn such complex tasks. However as the complexity of the task under investigation increases, representing the whole relationship in one single model using only raw sensory inputs would lead to large models. Training such models is extremely difficult, and, furthermore, obtained models often exhibit poor performances.**

This paper presents a bootsrapping method of generating complex robot training tasks using simple NARMAX models. We model the desired task by combining predefined low level sensor motor controllers.

The viability of the proposed method is demonstrated by teaching a *Scitos G5* autonomous robot to achieve complex route learning tasks in the real world robotics experiments.

I. Introduction

One approach to generating controllers for robotics sensor-motor tasks, using non-linear mapping techniques, can be summarized as follows: The programmer demonstrates the desired behaviour to the robot by driving it manually in the target environment. During this run, the sensor preception and the desired velocity commands of the robot are logged. Having thus obtained training data, the sensor based control models — which link the perception of the robot to the desired motor commands to achieve the desired task — are obtained using non-linear mapping techniques ([Demiris and Hayes, 1996] [Nehmzow et al., 2005], [Akanyeti et al., 2007a]) (see figure 1). Single model is usually enough to identify the whole relationship successfully.

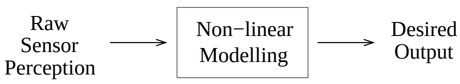

Fig. 1. The general approach to generate controllers for sensor-motor tasks.

This approach has been extensively used by the mobile robotics community and some good results have been achieved in many different mobile robotics applications ([Nguyen and Widrow, 1990], [Pomerleau, 1993], [Akanyeti et al., 2007b]). However as the complexity of the task under investigation increases, trying to represent the task in a single model, using only raw sensory inputs would lead to large models with many parameters to fit. Obtaining such models is difficult and usually such models exhibit poor performances.

[1]Dept. of Computing and Electronic Systems, University of Essex, UK
[2]School. of Computing and Intelligent Systems, University of Ulster, UK
[3]Dept. of Automatic Control and Systems Engineering, University of Sheffield, UK

Therefore it is common that the raw input readings are pre-processed with the aid of the programmer in order to decrease the dimensionality of the input space, and to extract higher level information from the sensory data in order to simplify the problem to certain extent. However preprocessing tenders the system identification process programmer dependent, which can result in brittle models.

A. Generating Complex Tasks by Bootstrapping

We argue that it is important to have a formal, algorithmic method to extract high level input information, minimizing the use of human knowledge. In this paper we therefore propose a bootstrapping behaviour generation method which uses low level behaviours to generate more complex ones. The method has three phases:

Phase 1: For obtaining simple sensor-motor controllers, we use the main modelling approach given in (figure 1) [Akanyeti et al., 2007a]. Some examples of such low level reactive-controllers are obstacle-avoidance, door traversal, wall-following, etc.

Phase 2: The controllers obtained at phase 1 are loaded to the robot in order to form a behaviour repertoire in the robot's memory. For more complex tasks, we obtain a model using the NARMAX system identification methodology, which models the new task as a function of these previously acquired behaviours. Here, the composition of behaviours is done using state variables which contain information about the state of the environment and the robot (see figure 2).

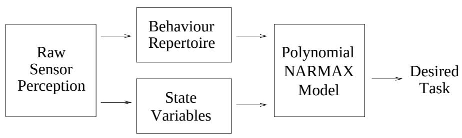

Fig. 2. The bootstrapping method of generating complex robot training tasks.

Phase 3: Once we obtain the model, we test it on the robot in order to validate performance. If the new controller is successfull it is added to the repertoire so that it can be used to generate even higher level controllers in the future.

II. ARMAX/NARMAX Modelling and Experimental Setup

a) Modelling Procedure: ARMAX (Auto-Regressive Moving Average models with eXogenous inputs) [Eykhoff, 1974], [Eykhoff, 1981] and NARMAX (Nonlinear ARMAX) [Chen and Billings, 1989], [Billings and Chen, 1998] modelling approaches are supervised parameter estimation methodologies for identifying both the important model terms and the parameters of unknown non-linear dynamic systems. These produce linear or nonlinear polynomial functions that model the relationship between some input and some output, both pertaining to the robot's behaviour. A more detailed discussion of about the modelling technique is presented in [Korenberg et al., 1988], [Billings and Voon, 1986].

b) Experimental Setup: The experiments described in this paper were conducted in the 100 square meter circular robotics arena of the University of Essex, using a *Scitos G5* mobile robot called *FOX*. The robot is equipped with a HOKUYO laser range finder. This sensor has a 4 m distance range, 240° angular range and approximately 0.36° angular resolution. The robot also incorporates a colour video camera with 640×480 pixels resolution which can deliver colour images up to 60Hz.

III. Simple Behaviour 1: Obstacle Avoidance

In the first experiment, we trained *FOX*, to avoid obstacles towards the "obvious" side as shown in figure 3; if robot has more space on the right side, it turns to right, and if there is more space on the left, it turns to left.

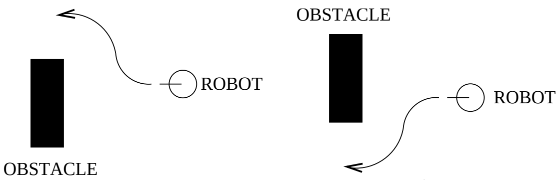

(a) (b)

Fig. 3. Experiment 1. The desired obstacle avoidance behaviour. The robot must choose the "obvious" side to avoid the obstacle in front. While approaching to the boxes if robot has more space on the right side, it turns right (b) and if there is more space on the left, it turns to the left (b).

In order to teach the desired behaviour to *FOX*, the programmer drove the robot in the training environment (figure 4) avoiding obstacles by turning the robot to the side having more space. During the experiments, the robot was started from the initial position S and stopped at the destination point F for 16 times. During each run, laser readings and the motor commands of the robot were logged in every 250 ms.

Having obtained the training data, we coarse coded laser readings into 11 sectors by averaging 62 readings for each 22° intervals. Coarse coded laser readings were clipped at 1.5m to avoid models taking far-away obstacles into account that are irrelevant to obstacle avoidance.

We then modelled the angular velocity ω_o of the robot as a function of coarse coded laser readings $(u_1 - u_{11})$ using ARMAX system identification methodology where the initial training parameters were $N_u = 0$, $N_y = 0$ and $l = 1$. The obtained model was a linear polynomial with 6 terms (table I).

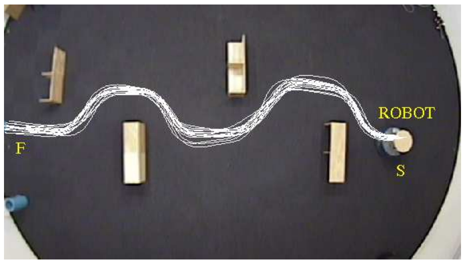

Fig. 4. Experiment 1. The trajectory of the robot guided by the programmer. The robot was started from point S and avoided boxes along the route until it reaches the destination point F. The experiment was repeated 16 times and for each run the laser readings and the motor commands of the robot were logged in every 250ms. Note that trajectories of the robot was obtained using a *Vicon* motion tracking system mounted in the arena which can deliver 3D data upto 100Hz with an accuracy better than 1mm.

$$\begin{aligned} \omega_o(n) &= +0.183 - 0.187 \cdot u_4(n) - 0.137 \cdot u_5(n) \\ &\quad -0.021 \cdot u_6(n) - 0.045 \cdot u_7(n) + 0.265 \cdot u_8(n) \end{aligned}$$

TABLE I

Experiment 1. The ARMAX model linking the laser perception to the angular velocity of the robot for avoidance behaviour.

c) Model validation: We tested the steering speed model on the robot in three different test environments. During the experiments the linear speed of the robot was clamped to 0.1m/s.

In the first test environment, the robot was started from 20 different initial positions in front of two boxes put next to each other and was expected to avoid them from the "obvious" side where the robot had more space. The results (figure 5(a)) confirmed the expectation where the robot was able to avoid obstacles as desired.
[1]

(a) (b) (c)

Fig. 5. Experiment 1. The three environments where the obtained angular speed model ω_o given in table I was tested for obstacle avoidance behaviour. The results show that ω_o was captured the general relationship between the laser perception and the motor commands of the robot to achieve the obstacle avoidance behaviour.

In the second (figure 5(b)) and third (figure 5(b)) test

[1] In three runs out of 20, when the robot was started from the mid-point of the two boxes facing towards them, the robot was not able to choose a side and failed to escape from the boxes. One possible solution to this problem would be to train a linear speed model as well which exponentially decreases as the robot comes closer to the boxes, but for the purpose of the work described in this paper the achieved results were enough.

environments, we tested if the obtained angular speed model captured the real essence of obstacle avoidance behaviour. The robot was started in front of the boxes arranged to simulate a right and a left corner and in both cases the robot was successfull to avoid the corners by turning the “obvious” side. Note that for both environment the robot was started from 16 different initial positions.

IV. Simple Behaviour 2: Left/Right Turning according to the Colour of the Obstacle

In the second experiment, we trained *FOX* in such a way that it determined the turning direction according to the colour of the obstacle rather than choosing the “obvious” side. The experimental scenario here is: while *FOX* approaches to an obstacle, it identifies the colour of the obstacle by a simple colour filtering algorithm, then i) if the colour of the obstacle is red, the robot avoids the obstacle by turning to right, and ii) if the colour of the obstacle is green, the robot escapes the obstacle by turning to left.

In order to obtain the training data set, we drove the robot in two environments: i) the first one contained boxes of red colour, where the robot was avoiding them by turning to right (figure 6(a)) and ii) the second environment contained green boxes where the robot was avoiding them by turning to left (figure 6(b)). In each environment, we conducted the experiments 10 times starting the robot from initial point S, stopping at the final point F.

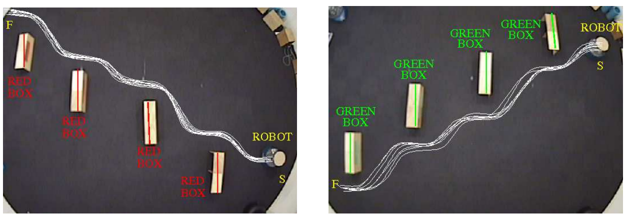

(a) (b)

Fig. 6. Experiment 2. The trajectories of the robot in two training environments; i) the first one contained boxes with red colour where the robot was avoiding them by turning to right (a) and ii) the second environment contained green boxes where the robot was avoiding them by turning to left (b))

During the experiments, we logged the coarse coded laser readings and the motor responses of the robot as well as the colour index c_i ($c_i = 1$ for green, $c_i = 2$ for red boxes) of the closest obstacle to the robot every 250 ms.

After logging this perception-action data, we modelled the angular speed ω_t of the robot using NARMAX system identification methodology as a function of the coarse coded laser readings ($u_1 - u_{11}$) and the colour index of the detected obstacle (c_i). The initial training parameters were $N_u = 0$, $N_y = 0$ and $l = 2$ and the resultant NARMAX model contained 21 terms (table II).

The resultant polynomial model ω_t is essentially the combination of two polynomials, where each polynomial turns the robot to a different direction, and the transition between the two is performed using the terms including state variable c_i (the last two rows in table II).

$$
\begin{aligned}
\omega_t(n) \; = \; & +3.839 - 0.661 \cdot u_4(n) - 0.212 \cdot u_5(n) \\
& +0.650 \cdot u_7(n) - 2.413 \cdot u_8(n) - 0.093 \cdot u_4(n)^2 \\
& +0.150 \cdot u_5(n)^2 - 0.002 \cdot u_7(n)^2 + 0.050 \cdot u_8(n)^2 \\
& -0.202 \cdot u_4(n) \cdot u_5(n) - 0.098 \cdot u_4(n) \cdot u_6(n) \\
& -0.546 \cdot u_4(n) \cdot u_7(n) + 1.121 \cdot u_4(n) \cdot u_8(n) \\
& -0.249 \cdot u_5(n) \cdot u_6(n) + 0.076 \cdot u_5(n) \cdot u_7(n) \\
& -0.129 \cdot u_6(n) \cdot u_7(n) + 0.130 \cdot u_6(n) \cdot u_8(n) \\
& -1.469 \cdot c_i(n) + 0.263 \cdot c_i(n) \cdot u_5(n) \\
& +0.369 \cdot c_i(n) \cdot u_6(n) + 0.280 \cdot c_i(n) * u_7(n)
\end{aligned}
$$

TABLE II

Experiment 2. The NARMAX model for the angular speed of the robot. The model is a second order polynomial including 18 terms. The last two rows show the terms including state variable c_i.

d) Model validation: As before we validated the performance of the obtained angular speed model by testing it on the robot. We put the robot in front of red and green boxes and let the model drive the robot. For each coloured box, the model was tested 16 times and the resultant trajectories of the robot are given in figure 7. They confirm that the model given in table II achieves the desired behaviour.

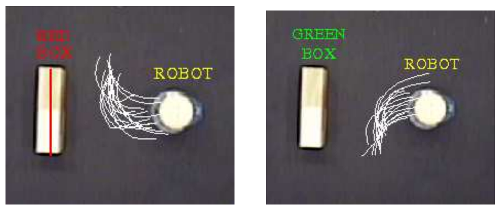

(a) (b)

Fig. 7. Experiment 2. The resultant trajectories of the robot guided by the angular speed model ω_t when it is confronting the: (a) red coloured boxes and (b) green coloured boxes. The results show that the obtained angular speed model was successful making the robot to turn the right direction according to the colour of the detected obstacle.

In order to quantify the performance of the angular speed model ω_t, we computed the strength of the association between the colour of the detected obstacle and the direction of the corresponding turning speed of the robot using *Cramer's V* test. To do so, we checked the sign of the resultant turning speed according to the colour of the detected obstacle during the test runs. When the robot detected a green obstacle, the resultant $\omega_t > 0$ (indicating to turn left) 97.651% of the time, and when the detected obstacle is red, $\omega_t < 0$ (indicating to turn right) 98.837% of the time. The results showed that there is a significant correlation where $V = 0.96$. Note that V varies between 0 and 1 corresponding to no association and perfect association respectively.

V. Complex Behaviour 1: Route Learning

The previous experiment demonstrates how different behaviours can be embodied in a single polynomial where the transition between behaviours is done using state variables containing information about the current state of the environment. We will now show that this can be used to achieve more complex tasks.

Scaling up from the first two experiments, the third task was to generate a polynomial which can guide *FOX* to follow a particular route in order to reach a desired object. The experimental scenario is given in figure 8, the environment is populated with red and green boxes in order to guide the robot to the destination point F, where the target object, blue pillar, is present.

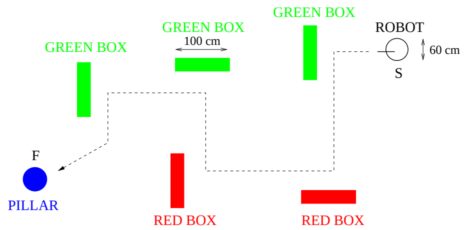

Fig. 8. Experiment 3. The experimental scenario where the desired task is to teach the robot to follow a particular route in order to reach the blue pillar. Note that the environment is populated with red and green boxes to indicate the right direction to the robot to follow.

To collect the training data, the programmer drove the robot manually in the target environment (figure 9) 10 times starting the robot from the initial position S and stopping the robot in front of the blue pillar (destination point F). During the training, laser readings, camera images and the motor commands of the robot were logged in every 250 ms.

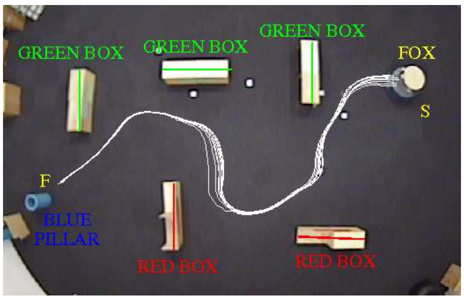

Fig. 9. Experiment 3. The trajectories of the robot guided manually by the human operator in order to obtain the training data.

A. Bootstrapping from Low-Level Controllers

After logging the training data, as discussed in section I-A, we processed the laser readings and the raw images to extract three low level controllers which will then be fed to polynomial NARMAX models as inputs. These controllers are:

- **Obstacle avoidance controller** The first controller in the behaviour repertoire guides the robot to avoid obstacles. Here we used the polynomial model ω_o given in table I obtained in experiment 1 (section III).
- **Colour encoded turning controller** The second one turns the robot to right if the colour of the detected object is red and it turns the robot to left if the colour is green. Here we used the polynomial model ω_t given in table II, obtained during experiment 2 (section IV).
- **Object seeking controller**: We also implemented a simple object seeking controller which looks for the nearest object in front of the robot and guides the robot towards it.

Having identified the controllers, we also obtained three state variables which will help the system identification process to link the low level controllers in order to achieve the desired task:

- $\mathbf{d}_i$ defines if the target object is detected or not; $d = 0$ represents target object is not detected, and $d_i = 1$ represents target object is detected.
- $\mathbf{o}_i$ defines if there is an obstacle close to the robot; $o_i = 0$ represents there is no obstacle detected, and $o_i = 1$ represents the presence of an obstacle.
- $\mathbf{c}_i$ states the colour of the detected obstacle; $c_i = 1$ represents green, $c_i = 2$ represents red, and $c_i = 0$ represents all other colours.

e) Obtaining Polynomial Models: We then obtained two polynomial models; one for the linear speed v_r and one for the angular speed ω_r of the robot — as a function of the predefined behaviours (ω_o, ω_t and ω_w) and the state variables (d_i, o_i and c_i). The obtained models are given in table III.

$$
\begin{aligned}
v_r(n) &= +0.100 - 0.100 \cdot d_i(n) \\
\omega_r(n) &= +0.100 \cdot d(n) + 1.000 \cdot \omega_w(n) \\
&\quad -1.000 \cdot o_i(n) \cdot \omega_w(n) + 1.000 \cdot o_i(n) \cdot \omega_o(n) \\
&\quad -1.000 \cdot o_i(n) \cdot c_i(n) \cdot \omega_o(n) + 1.000 \cdot o_i(n) \cdot c_i(n) \cdot \omega_t(n) \\
&\quad +1.000 \cdot d_i(n) \cdot o_i(n) \cdot \omega_w(n) - 1.000 \cdot d_i(n) \cdot o_i(n) \cdot \omega_o(n) \\
&\quad +1.000 \cdot d_i(n) \cdot o_i(n) \cdot c_i(n) \cdot \omega_o(n) \\
&\quad -1.000 \cdot d_i(n) \cdot o_i(n) \cdot c_i(n) \cdot \omega_t(n)
\end{aligned}
$$

TABLE III

EXPERIMENT 3. THE POLYNOMIAL MODELS FOR THE LINEAR v_r AND ANGULAR SPEED ω_r OF THE ROBOT.

f) Models Validation: Having obtained the perception models v_r and ω_r, we tested them on the robot. We let the models drive the robot in the target environment 10 times. Figure 10 shows the resultant trajectories, where in each run the robot was successful to reach the target object.

VI. EXTENDED BOOTSRAPPING METHOD

In experiment 3 we have demonstrated how simple NARMAX models can be used to achieve more complex tasks. One interesting question here is "what happens if the low level controllers found in the behaviour repertoire are not adequate to generate the desired task?"

To address this question, we extended the proposed method by adding raw sensory perception to the modelling process. In this way, we let the polynomial model combine raw sensory data with the low-level controllers automatically. Again, transition between the controllers and the raw sensory

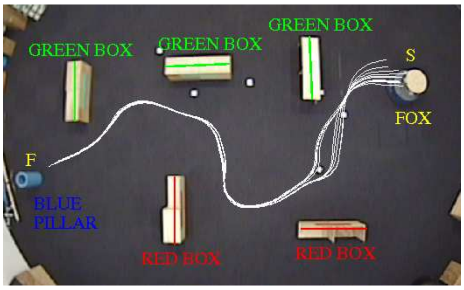

Fig. 10. Experiment 3. The trajectories of the robot under the control of the perception models given in table III. The results show that the robot successfully reached the target object in each run.

data is controlled according to the state of the environment and the robot (figure 11).

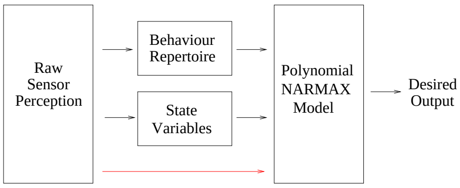

Fig. 11. The extended bootstrapping method of generating complex robot training tasks. In the extended version we also give raw sensory data as inputs to the system.

A. Complex Behaviour 2: Modelling Complex Route Learning Task

To demonstrate the extended method, we taught *FOX* to follow a complex route of different stages (figure 12). First, the robot has to reach a blue pillar by correctly following the coloured objects. Once it reaches the pillar, it has to wait with zero linear and angular speeds until the pillar is removed from the environment (stage 2). Once the pillar is removed, the robot must complete the route by traversing the two consecutive door-like openings with 1 m wide each to reach the destination point F.

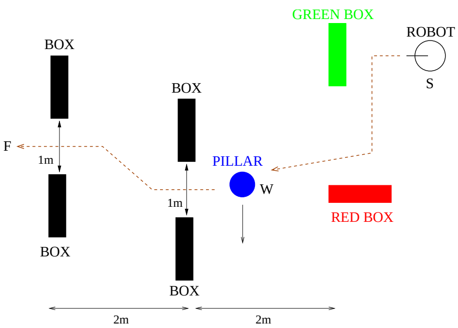

Fig. 12. Experiment 4. The experimental scenario for the desired complex route learning task.

As before we obtained the training data by driving the robot manually in the target environment shown in figure 13. Starting the robot at initial position S, first we drove the robot to point W. Then the robot was stopped in front of the pillar until the pillar was removed by the human operator. We then continued driving the robot to pass through two consecutive door-like openings. The experiments were repeated 10 times and for each run we logged the laser perception, camera images and the motor commands of the robot in every 250 ms.

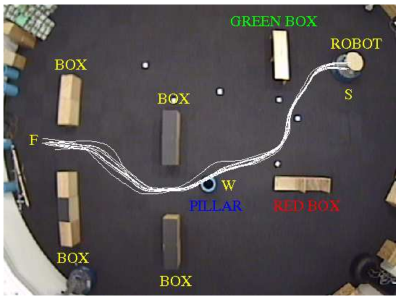

Fig. 13. Experiment 4. The trajectories of the robot under the manual control of the human operator training data collection.

g) Obtaining Sensor Based Models: After logging the training data, we fed the raw perception data to low-level controllers present in the behaviour repertoire of the robot to generate higher level inputs for the desired task. But this time we also coarse coded the laser readings into 11 sectors (u_1 to u_{11}) by averaging 62 readings for each 22° in order to enrich the system inputs, since there is no ready door traversing controller in the behaviour repertoire of the robot. Also for the transition between the behaviours, we computed a state flag s_i which indicates if the blue pillar is removed from the front of the robot ($s_i = 1$) or not ($s_i = 0$).

We then obtained two polynomial models v_c and ω_c using NARMAX system identification methodology as a function coarse coded laser readings ($u_1 - u_{11}$), route following controllers v_r and ω_r obtained in section V, and state variable s_i. The obtained models are given in table IV.

$$
\begin{aligned}
v_c(n) &= v_r + 0.1 \cdot s_i(n) \\
\omega_c(n) &= -0.033 + 1.016 \cdot \omega_r(n) + 0.144 \cdot u_4(n) \\
&\quad -0.088 \cdot u_5(n) + 0.004 \cdot u_6(n) - 0.131 \cdot u_7(n) \\
&\quad +0.014 \cdot u_8(n) + 0.208 \cdot \omega_r^2(n) - 0.026 \cdot u_4^2(n) \\
&\quad +0.029 \cdot u_5^2(n) + 0.062 \cdot u_7^2(n)^2 - 0.025 \cdot u_4(n) \cdot u_8(n) \\
&\quad +0.394 \cdot s_i(n) - 1.051 \cdot s_i(n) \cdot \omega_r(n) \\
&\quad -0.145 \cdot s_i(n) \cdot u_4(n) - 0.060 \cdot s_i(n) \cdot u_5(n) \\
&\quad -0.040 \cdot s_i(n) \cdot u_6(n) + 0.026 \cdot s_i(n) \cdot u_7(n)
\end{aligned}
$$

TABLE IV

EXPERIMENT 4. THE POLYNOMIAL MODELS FOR THE LINEAR AND ANGULAR SPEED OF THE ROBOT FOR COMPLEX ROUTE LEARNING BEHAVIOUR. THE LAST THREE ROWS SHOW THE TERMS INCLUDING STATE VARIABLE s_i.

h) Models Analysis and Validation: Once we obtained the sensor based models, we used them drive the robot in the target environment in order to validate the performance. Figure 14 shows the trajectories of the robot for 10 runs, where the robot completed the track successfully in each attempt.

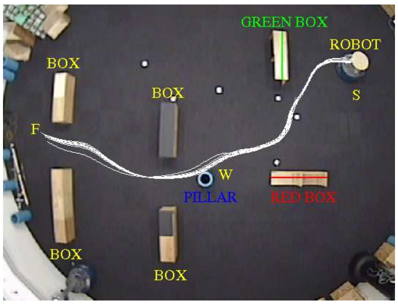

Fig. 14. Experiment 4. The trajectory of the robot under the control of the perception models given in table IV. The experiments were repeated 10 times and for each run the robot completed the track successfully to reach the destination point F without bumping into the boxes in each attempt.

Transparent Models: Having transparent models like the ones given in table IV has a number of advantages, for example the possibility to analyse the robot behaviour formally. Here, for instance, one can see that the model of table IV ω_c has two components. The first one is the colour based route following behaviour which was previously obtained in section V, taking the control of the robot when state flag s_i equals 0. The second behaviour is a door traversal controller activated when $s_i = 1$.

The separability of the behaviours enabled us to add door traversal controller to the behaviour repertoire of the robot. In this way we do not only obtain models to achieve the desired task, but we also extract new low level controllers from the polynomial model in order to enrich the behaviour repertoire of the robot.

VII. Conclusion and Future Work

This paper introduces a bootstrapping method of generating complex robot training tasks using polynomial NARMAX structures. The method is based on obtaining hierarchical polynomial models which model the desired task by combining predefined low level sensor motor controllers and raw sensory data in a judicious way.

The method uses the advantage of polynomial models being truly linear in the parameters [Chen et al., 1990]. This allows us to combine different low level controllers in a single polynomial in order to achieve more complex tasks. The transition between these controllers is done using state variables which contain information about the state of the environment.

Acknowledgments

We express our thanks to Emre Özbilge for his contribution to this paper. We also gratefully acknowledge that the RobotMODIC project is supported by the Engineering and Physical Sciences Research Council under grant GR/S30955/01.

References

[Akanyeti et al., 2007a] Akanyeti, O., Kyriacou, T., Nehmzow, U., Iglesias, R., and Billings, S. (2007a). Visual task identification and characterisation using polynomial models. *Robotics and Autonomous Systems*.

[Akanyeti et al., 2007b] Akanyeti, O., Nehmzow, U., Weinrich, C., Kyriacou, T., and Billings, S. (2007b). Programming mobile robots by demonstration through system identification. In *ECMR*, Freiburg, Germany.

[Billings and Chen, 1998] Billings, S. and Chen, S. (1998). The determination of multivariable nonlinear models for dynamical systems. In Leonides, C., (Ed.), *Neural Network Systems, Techniques and Applications*, pages 231–278. Academic press.

[Billings and Voon, 1986] Billings, S. and Voon, W. S. F. (1986). Correlation based model validity tests for non-linear models. *International Journal of Control*, 44:235–244.

[Chen and Billings, 1989] Chen, S. and Billings, S. (1989). Representations of non-linear systems: The narmax model. *International Journal of Control*, 49:1013–1032.

[Chen et al., 1990] Chen, S., Billings, S. A., Cowan, C. F. N., and Grant, P. M. (1990). Practical identification of narmax models using radial basis functions. *International Journal of Control*, 56:6:1327–1350.

[Demiris and Hayes, 1996] Demiris, J. and Hayes, G. (1996). Imitative learning mechanisms in robots and humans. In *Proc. 5th European Workshop on Learning Robots*, pages 9–16, Bari, Italy.

[Eykhoff, 1974] Eykhoff, P. (1974). *System Identification: parameter and state estimation*. Wiley-Interscience, London.

[Eykhoff, 1981] Eykhoff, P. (1981). *Trends and Progress in System Identification*. Pergamon Press.

[Korenberg et al., 1988] Korenberg, M., Billings, S., Liu, Y. P., and McIlroy, P. J. (1988). Orthogonal parameter estimation algorithm for non-linear stochastic systems. *International Journal of Control*, 48:193–210.

[Nehmzow et al., 2005] Nehmzow, U., Kyriacou, T., Iglesias, R., and Billings, S. (2005). Self-localisation through system identification. In *Proc. of ECMR 05 - European Conference on Mobile Robots 2005*. Springer Verlag.

[Nguyen and Widrow, 1990] Nguyen, D. and Widrow, B. (1990). The truck-backer upper: An example of self-learning in neural networks. *IEEE Control Systems Magazine*, 10:2:18–23.

[Pomerleau, 1993] Pomerleau, D. (1993). *Neural Network Vision for Robot Driving*.